Shape Optimization of Connector Contacts for Reduced Wear and Reduced Insertion Force

Jochen Horn
Bernhard Egenolf
AMP Deutschland GmbH

ABSTRACT

Concept and formulas are presented for predicting optimized shapes of pin and socket spring at the entry portion of a connector. The results are reduced insertion force and wear caused by friction during mating. A particular advantage of the method is that changes of existing designs require minor shape modifications only of the regions where pin and socket slide against each other during insertion.

INTRODUCTION

Reducing insertion force and wear are among the goals of optimization of pin and socket connectors with a contact spring. Previous efforts concentrated almost entirely on development of improved coatings applied to the contact surfaces. Departing from the conventional approaches, this paper concentrates on the effect of the pin and socket's shape on insertion force and wear. Of particular importance in this regard are special geometries of the pin tip and the socket entry.

GENERAL APPROACH

To accomplish smooth and easy formation of the contact, the pin is pointed and enters funnel-shaped socket springs. During insertion, the pin and socket slide along each other, whereby a force component essentially normal to the direction of insertion evolves. This force loads the springs. The deflected springs then produce the contact force required for the electrical connection. Because of the sliding motion and the finite value of the force acting normal to the contacting surfaces, wear occurs at these surfaces.

Two Cartesian systems of coordinates $\{X_s, Y_s\}$ and $\{X_f, Y_f\}$ where the first is fixed to the pin, the second to the socket are introduced. Both move relative to an external system fixed in space in which the insertion distances is measured. The schematics shown in Figures 1 and 2 offer the means to optimize the set of geometric parameters $Y_s(X_s)$ and $Y_f(X_f)$ for pin and socket springs. The subscripts s and f indicate pin *(Stift)* and spring *(Feder)*, respectively. A comparison of the force components yields for the insertion force F_s as function of the insertion distance s

$$F_s = \frac{F_f(x(s)) \cdot \cos(\beta_b(s) - \beta_0) \cdot [\sin(\alpha(s)) + \mu \cdot \cos(\alpha(s))]}{\cos(\alpha(s) + \beta_b(s)) - \mu \cdot \sin(\alpha(s) + \beta_b(s))}; \qquad (1)$$

with

$F_f = F_f(x)$ = spring force;
$x(s)$ = spring deflection;
s = insertion distance;
μ = coefficiant of dynamic friction;
$\alpha = \alpha(s)$ = angle between connector axis and tangent to surface of socket and spring at point of contact;
β_0 = angle between spring element and connector axis before insertion;
$\beta_b = \beta_b(s)$ = angle between connector axis and the line formed by connecting and actual contact point to the fixed point of the spring;

The angle α (s) is strongly determined by the shape of pin and socket. It depends also on the first derivatives $d(Y_s)/d(X_s)$ and $d(Y_f)/d(X_f)$, which are functions of the coordinates X_s and X_f, respectively.

The general behavior of the insertion force $F_s(s)$ is shown

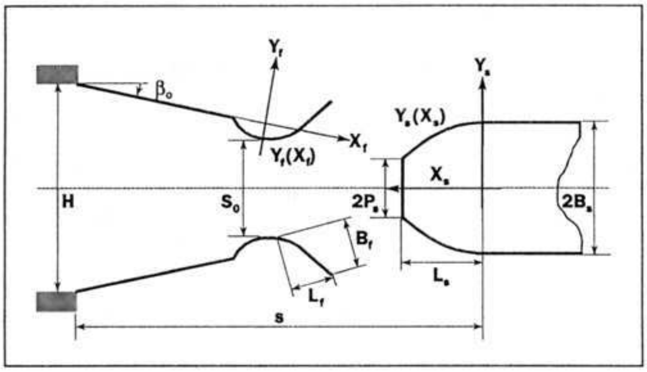

Figure 1. Schematic of contact model. H = width of socket, 2 · B, = width (diameter) of pin, 2. P_s = width (diameter) of tip of pin, L_s = length of pin taper, So = distance of spring before insertion.

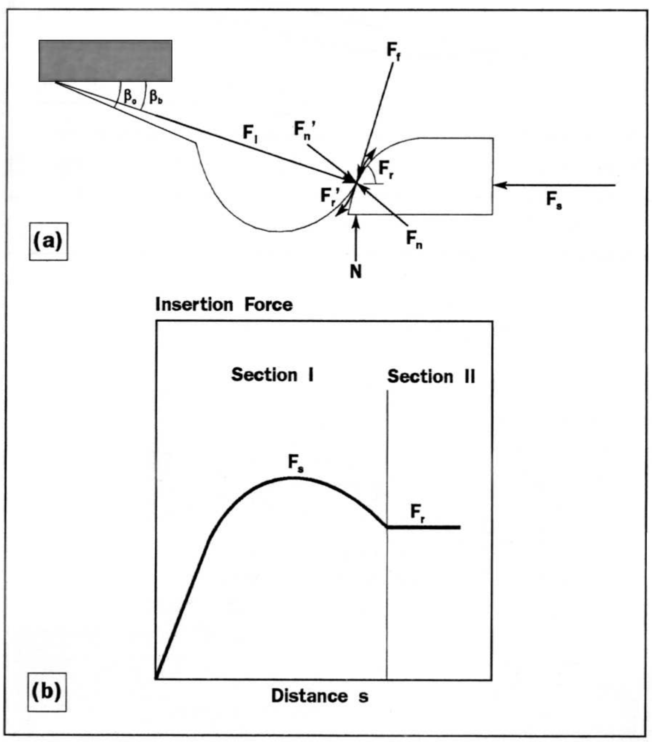

Figure 2. a) Illustration of force components during insertion, b) qualitative graphic representation of insertion force F_s as function of insertion distances. Section I would correspend to the load phase; section II to the wipe phase during insertion.

in Figure 2. As shown in detail in reference 1, variation of Ff(x(s)) and a(s) in equation (1) caused by variations of $Y_s(X_s)$ and $Y_f(X_f)$ indicates that the shape of the curve and its maximum depend critically on the geometry of the two contacts. This effect is used to design for reduced insertion force.

Contact pressure is a measure for stress causing wear in sliding friction between solids.[2-4] Wear increases with increasing contact pressure. The glide or sliding path of the connector contacts within the entry regions of spring and pin is, in either case, characterized by the contact pressure

$$p(s) = K \cdot P_c(s), \tag{2}$$

where

$$K = \sqrt{\frac{E}{2 \cdot \pi \cdot B \cdot (1 - \nu^2)}}, \tag{3}$$

$$P_c(s) = \sqrt{F_n(s) \cdot \left(\frac{1}{R_f(s)} + \frac{1}{R_s(s)}\right)}, \tag{4}$$

$$F_n(s) = F_f(x(s)) \left(\frac{\cos(\beta_b(s) - \beta_0)}{\cos(\alpha(s) + \beta_b(s)) - \mu \cdot \sin(\alpha(s) + \beta_b(s))}\right), \tag{5}$$

with

$R_s(s)$ = radius of curvature at point of contact of the pin surface;
$R_f(s)$ = radius of curvature at point of contact of the socket surface;
E = Young's modulus of the contact material;
ν = Poisson's ratio of the contact material;
B = width of contact.

The two radii of curvature $R_s(s)$ and $R_f(s)$ depend on the derivatives $d(Y_s)/d(X_s)$, $d^2(Y_s)/d(X_s)^2$, and $d(Y_f)/d(X_f)$, $d^2(Y_f)/d(X_f)^2$, respectively. These derivatives are functions of X_s and X_f, which, in turn, are determined by the original geometry of pin and socket. Therefore, the pressure p(s) in equation (2), including its peak value, depends also on geometric parameters of pin and socket at the entry region. Since the wear is determined by the pressure p(s) it can also be controlled by proper geometric design.

During insertion the position of the contact point at socket X_f and pin X_s is a function of the insertion distances:

$$X_f = X_f(s), \tag{6}$$

$$X_s = X_s(s), \tag{7}$$

so that the pressure at the surface of socket and pin is also a function of X_f and X_s:

$$p(X_f) = K \cdot P_c(X_f), \tag{8}$$

$$P(X_s) = K \cdot P_c(X_s), \qquad (9)$$

and is determined by equations (1) to (7).

A computer program permits numerical evaluation of equations (1) to (9) for various combinations of geometric parameters and functions $Y_s(X_s)$ and $Y_f(X_f)$. The most desirable set of them is then selected to meet the following requirements:

- Low level of insertion force,
- Low maximum pressure and uniform pressure distribution.

Not directly derived from the equations, a third requirement is introduced: Measured on the socket surface, the difference between the position where maximum pressure occurs and that of establishing the electrical contact should be large. This requirement results in reduced creep and also a reduction of displacement of particles generated by wear and the presence of corrosion products.

EXAMPLE

Without changing the main dimensions of pin and socket, a given connector was optimized regarding insertion force and pressure by modifying the shape of the two connector elements in the entry region. The original shapes are shown for the spring and the pin in Figures 3 and 4, respectively, as curves (l). To illustrate the changes, the contours of the mathematically derived optimum shapes are shown as curves (2) in the same figures.

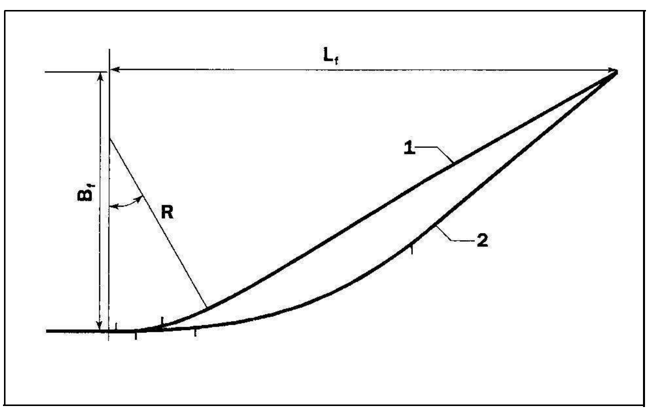

Figure 3. Contours of spring shape at entry portion: (1) original shape, (2) theoretically predicted optimized shape. For definition of L_f and B_f see Figure 1.

Introducing the geometric parameters of the original design and the optimized pin-socket combination in equation (1) and plotting $F_s(s)$ versus sin Figure 5, shows that the insertion force maximum is reduced by 30% relative to that of the original combination. A comparison of the four curves in the graph illustrates also that the change in the top geometry of the pin contributes most to the insertion-force reduction. Optimizing the spring shape only reduces $(F_s)_{max}$ by 11%, that of the pin only by 19%. A similar performance improvement is shown for the pressure $p(X_s)$ and $p(X_f)$ in Figure 6. Introducing the new entry shapes for pin and spring reduces by 70% the stress component responsible for sliding wear and flattens the entire p(X) -curve to a more uniform one. Again, the change of the pin shape contributes most to the improvement.

The validity of the optimization concept and the specific approach described here was tested experimentally. Figure 7 shows three different pin shapes used in this evaluation. Figure 8 shows the results by plotting the measured insertion force against the displacement distance s for the three different pins. The measurements confirm the theoretical predictions.

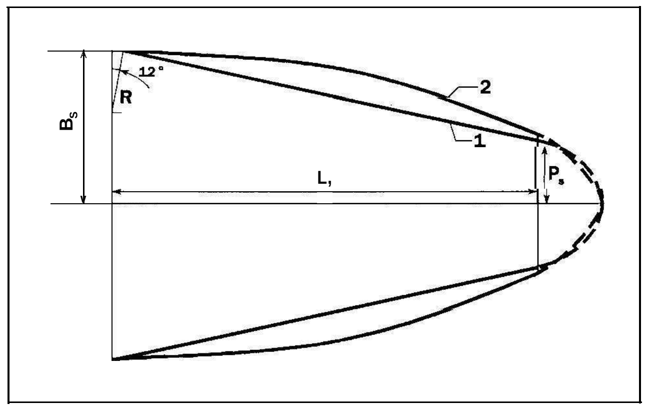

Figure 4. Contours of pin shape at entry portion: (1) original shape, (2) theoretically predicted optimized shape. For definition of L_s, P_s and B_s see Figure 1.

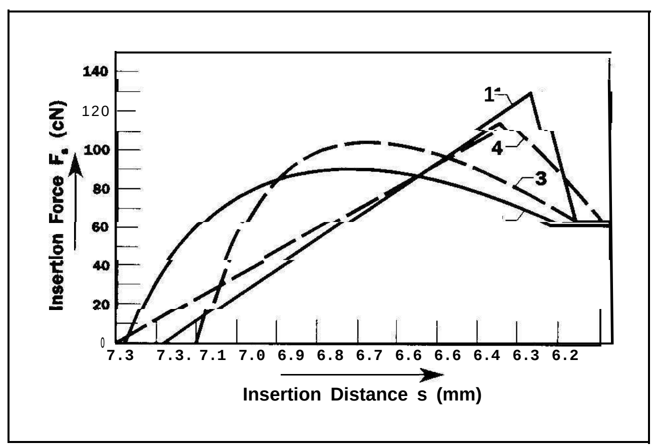

Figure 5. Computed insertion force $F_s(s)$ for different combinations of shapes of pin and spring: (1) original system, (2) optimized system, (3) original spring/optimized pin, (4) original pin/optimized spring.

One advantage of the concept of connector optimization by optimizing contact geometry at the entry region is that the optimized contacts can be used in the original system because the optimization does not require major dimensional changes of the connector parts. The minor changes made to correct the surface within a rather narrow range leaves the improved version compatible with the original one.

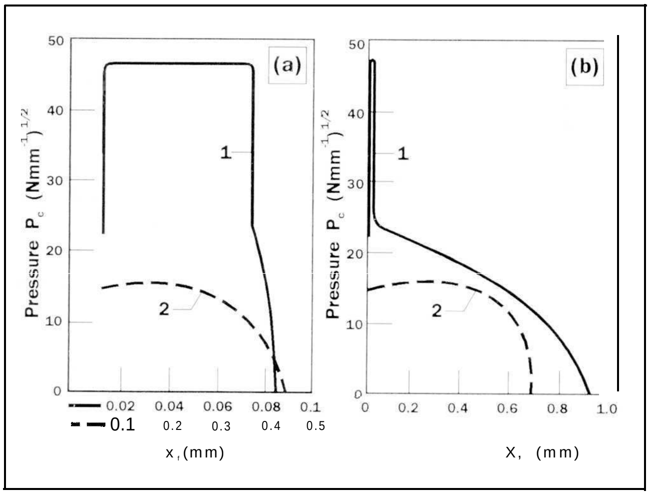

Figure 6. Computed value P_C (proportional to contact pressure) as function of **a)** X_f coordinate of the spring, **b)** X_s coordinate of the pin. In both, (1) is the original system and (2) is the optimized system.

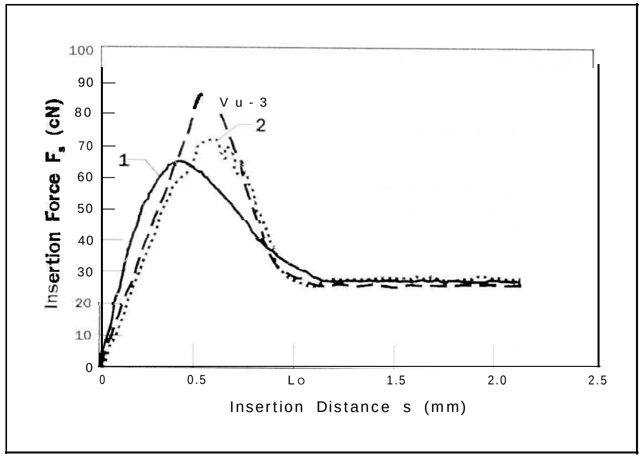

Figure 8. Measured insertion force $F_s(s)$ for pins of Figure 7: (1) optimized pin, (2) and (3) original, wedge-shaped pin.

CONCLUSIONS

The mathematical procedure for reducing insertion force and wear through optimization of the pin and socket spring shapes at the entry range offers a valuable design tool. The theory was confirmed experimentally and proven in manufacturing. In one actual case the insertion force of the connector with wedge-shaped pins was about 50 N. The new pin shape with optimized geometry at the top reduced the insertion force to about 20 N.

a b c

Figure 7. Illustration of shapes of pins: **a)** optimized pin, **b)** and **c**) original, wedge-shaped pin.

REFERENCES

1. *J. Horn, Mechanische Eigenschaften von Kontaktsystemen und Kontaktoberjlachen.* Dissertation B, Technische Universität Chemnitz, 1985.

2. I.W. Kragelski, *Reibung und Verschleiff* (Verlag Technik, Berlin, 1971), p. 170.

3. J.F. Archard, J. Appl. Physics 24,981 (1953).

4. R. Helm, *Electric Contacts: Theory and Applications,* Fourth Ed. (Springer Verlag, Berlin, 1967).

Jochen Horn is in the Engineering Department at AMP Deutschland GmbH in Langen, Germany.

Dr. Horn holds a diploma in physics from Technische Unuversität Dresden, a Dr. rer. nat. in 1976 and a Dr. sc.nat. in 1985 from Technische Universität Chemnitz. During 1966–88 he worked at the Technische Universität Chemnitz on physics of thin films. He authored or co-authored more than 40 articles. Since joining AMP in 1989, he has worked in the areas of contact physics, the characteristics and use of new finishes as well as base materials. He is a member of the Metal Finishing Working Group.

Bernhard Egenolf is Project Engineer in Automotive Product Engineering at AMP Deutschland GmbH, Langen, Germany.

B. Egenolf is Diplom-Ingenieur für Precision Engineering (1964) from Ingenieurschule (now named Fachhochschule) Frankfurt am Main. He worked at VDO, Frankfurt am Main, with thermo- and fuel sensors and at Honeywell, Dörnigheim, with electronic packaging. From Braun, Kronberg, he possesses patents for home appliances. He joined AMP in 1972 and was responsible for design and introduction of MT-Interconnectionsystem, MT-Edge and Timer-Connectors for washing-machines. Since 1984 he developed the well known Junior-, Standard- and Maxi-Power-Timer contacts.